Ecological Modelling 240 (2012) 29–40

Contents lists available at SciVerse ScienceDirect

Ecological Modelling

journal homepage: www.elsevier.com/locate/ecolmodel

Improving model parameter estimation using coupling relationships between vegetation production and ecosystem respiration

Wenping Yuan[a,b,*], Shunlin Liang[a,b,c], Shuguang Liu[d], Ensheng Weng[e], Yiqi Luo[e], David Hollinger[f], Haicheng Zhang[b]

[a] State Key Laboratory of Remote Sensing Science, Jointly Sponsored by Beijing Normal University and Institute of Remote Sensing Applications, Chinese Academic of Science, Beijing 100875, China
[b] College of Global Change and Earth System Science, Beijing Normal University, Beijing 100875, China
[c] Department of Geography, University of Maryland, College Park, MD 20742, USA
[d] Earth Resources Observation and Science Center, United States Geographical Survey, Sioux Falls, SD 57198, USA
[e] Department of Botany and Microbiology, University of Oklahoma, Norman, OK 73019, USA
[f] USDA Forest Service, Northern Research Station, Durham, NH 03824, USA

ARTICLE INFO

Article history:
Received 25 January 2012
Received in revised form 10 April 2012
Accepted 27 April 2012

Keywords:
Bayesian inversion
Eddy covariance
Markov chain Monte Carlo
Gross primary production
Ecosystem respiration
Parameter estimation

ABSTRACT

Data assimilation techniques and inverse analysis have been applied to extract ecological knowledge from ecosystem observations. However, the number of parameters in ecosystem models that can be constrained is limited by conventional inverse analysis. This study aims to increase the number of parameters that can be constrained in parameter inversions by considering the internal relationships among ecosystem processes. Our previous study has reported thermal adaptation of net ecosystem exchange (NEE). Ecosystems tend to transfer from a carbon source to sink when the air temperature exceeds the mean annual temperature, and attain their maximum uptake when the temperature reaches the long-term growing season mean. Because NEE is the difference between gross primary production (GPP) and ecosystem respiration (ER), the adaptation of NEE indirectly indicates the coupling relationship between GPP and ER. Five assimilation experiments were conducted with (1) estimated GPP based on eddy flux measurements, (2) estimated GPP and coupling relationship between GPP and ER, (3) observed NEE measurements, (4) observed NEE measurements and internal relationship between GPP and ER and (5) observed NEE, estimated ER and GPP. The results show that the inversion method, using only estimated GPP based on eddy covariance towers, constrained 4 of 16 parameters in the terrestrial ecosystem carbon model, and the improved method using both GPP data and the internal relationship between GPP and ER allowed us to constrain 10 of 16 parameters. The improved method constrained the parameters for ER without additional ER observations, and accordingly improved the model performance substantially for simulating ER. Overall, our method enhances our ability to extract information from ecosystem observations and potentially reduces uncertainty for simulating carbon dynamics across the regional and global scales.

1. Introduction

Ecosystem models have been relatively well developed and extensively applied to ecological research since the 1960s (Odum, 1956; Watt, 1966). Most of the major ecosystems and community processes have been incorporated into models (Parton et al., 1987; Rastetter et al., 1991; Ågren and Bosatta, 1998). A major source of model prediction errors has been partly attributed to unconstrained response functions and parameter values (Green et al., 1999; MacFarlane et al., 2000; Luo et al., 2003). Many parameters in ecosystem models are difficult or impossible to directly measure (Luo et al., 2001; Van Oijen et al., 2005). Various data-model assimilation and inverse analyses techniques have been used recently for parameter estimation in biogeochemical models, including gradient methods (Wang et al., 2001; Rayner et al., 2005), Kalman filter (Williams et al., 2005; Gove and Hollinger, 2006) and Markov chain Monte Carlo approach (Braswell et al., 2005; Knorr and Kattge, 2005).

However, almost all the parameter estimation studies have shown that the number of parameters that can be constrained is limited (Wang et al., 2001). For example, the analysis of the covariance matrix in the parameter estimation conducted by Wang et al. (2001) showed that only a maximum of 3 or 4 parameters could be

* Corresponding author at: College of Global Change and Earth System Science, Beijing Normal University, Beijing 100875, China. Tel.: +86 10 58807715.
E-mail address: wenpingyuancn@yahoo.com (W. Yuan).

0304-3800/$ – see front matter © 2012 Elsevier B.V. All rights reserved.
http://dx.doi.org/10.1016/j.ecolmodel.2012.04.027

determined independently from a short record of CO_2 flux observation. Multiple years of NEE data constrain 13 out of 23 parameters in a simplified photosynthesis and evapotranspiration (SIPNET) model using stochastic Bayesian inversion (Braswell et al., 2005). Six datasets of soil respiration, woody biomass, foliage biomass, litterfall and soil carbon content from the Duke Forest free-air CO_2 enrichment experiment (FACE) were able to constrain 4 out of 7 carbon transfer coefficients at ambient CO_2 and 3 at elevated CO_2 (Xu et al., 2006). This situation has been identified as a major source of uncertainty in model prediction (Schulz et al., 2001).

Whether some model parameters can be well constrained by the data depends upon the amount and quality of information in the measurements. Santaren et al. (2007) found that model parameters related to photosynthesis and energy partitioning are well resolved by eddy flux measurements, whereas model parameters related to respiration are poorly resolved due to limited information about respiration processes included within eddy flux measurements. The assimilation experiments showed that only biometric data effectively constrain carbon transfer coefficients from plant pools in leaves, roots, and wood, and that more coefficients were constrained when using both biometric and NEE data because NEE provided the information about other carbon pools such as litter, microbial biomass, and SOM pools, from which CO_2 was released (Zhang et al., 2010). Using multiple-constraint model data assimilation (MCMDA) methods which combines the observations from multiple sources such as biometry, eddy covariance tower, and remote sensing in such a way as to maximize consistency among all datasets simultaneously, has become an effective procedure for estimating model parameters (Wang and Barrett, 2003; Wang and McGregor, 2003; Richardson et al., 2010).

Although combinations of various observations can effectively improve the parameter information, shortcomings unfortunately exist in the multiple-constraint method. Ecosystem models include almost all physiological processes which range across hourly, daily, monthly, yearly even century timescales; additionally, these processes occur within one or more ecosystem components (e.g., soil, atmosphere, and vegetation). However, few sites can conduct the measurements for nearly all ecosystem variables, and most ecosystem observations require a great deal of time and energy.

Moreover, recognition is growing of the impacts of the uncertainties inherent in these measurements (Hollinger and Richardson, 2005). In the context of model-data fusion, Raupach et al. (2005) argue that measurement errors are as important as data values themselves because the specification of data uncertainties will affect not only the uncertainty of the model, but also the model predictions. Model-data fusion experiments showed measurement errors had significant effects on the probability distribution function of parameters, which means they affected information retrieval and the uncertainties of predicted variables increased with increase of measurement errors (Weng and Luo, 2007).

Similarly with various observations, interior relationships among physiological processes within an ecosystem also provide important information about various ecosystem processes. For example, plant stomatal conductance determines both diffusion of CO_2 into the leaf and diffusion of water vapor. Leaf level measurements have demonstrated the strong correlation between carbon assimilation and transpired water and the ratio of carbon assimilation to transpiration is a function of vapor pressure deficit (VPD), which is consistent across various ecosystem types (Beer et al., 2009). However, to our knowledge, the estimate of model parameters using the interior ecosystem processed relationships has still not been investigated. This study was designed to assess the impact of the interior coupling relationship between photosynthesis and respiration on model parameter inversion.

2. Method and data

2.1. Data source

We used eddy covariance (EC) measurements from the AmeriFlux site at Howland, ME, USA, in our inverse analysis. The flux site is located in a mid-latitude coniferous forest ecosystem (45.20°N, 68.74°W). The forest is unmanaged and described in detail in other publications (Hollinger et al., 1999, 2004). The five datasets from 2000 to 2005 used to derive optimized parameter values are estimated gross primary production (GPP) and ecosystem respiration (ER) based on EC measurements of CO_2 flux, air temperature at canopy top (T_a), photosynthetically active radiation (PAR), relative humidity (RH), and leaf area index (LAI) derived from the MODIS (MODerate Resolution Imaging Spectroradiometer) LAI product. Among them, daily GPP, ER, NEE, T_a, PAR, and RH were taken directly from the eddy tower; whereas, daily LAI data were interpolated from 8-day measurements. ER was estimated from 2nd order Fourier regressions between Julian day and nocturnal respiration when the friction velocity (u^*) exceeded 0.2 m s^{-1} (Hollinger et al., 2004; Richardson et al., 2006). This method is not sensitive to diurnal (hourly) changes in respiration. GPP was calculated as the difference between NEE and ER. No attempt was made to fill the data gaps. Daily values were excluded when missing hourly data represented >20% of the time on a given day (Yuan et al., 2009).

2.2. Model description and parameters

The model used here is a flux-based ecosystem model (FBEM) (Wu et al., 2009), which is fully described with equations in Appendix. In brief, the FBEM describes the short-time processes of GPP and ER as regulated by environmental variables. Canopy photosynthesis was estimated from LAI and leaf photosynthesis (Sellers et al., 1992). The latter was described using the model developed by Farquhar et al. (1980) for both carboxylation and electron transport process together with a stomatal conductance model (Leuning, 1995; van Wijk et al., 2000; Chang, 2003). Ecosystem respiration was modeled by a function of temperature with the widely used Q_{10} function (Van't Hoff, 1899). Net ecosystem exchange of CO_2 to the atmosphere (NEE) was calculated by:

$$\mathrm{NEE} = \mathrm{GPP} - \mathrm{ER} \quad (1)$$

In total, there were 16 parameters that governed the model's behavior (Table 1, Appendix).

2.3. Thermal adaptation of net ecosystem exchange

All ecosystem models for predicting NEE use separate algorithms to describe the changes of GPP and ER with temperature (Running and Coughlan, 1998; Running and Gower, 1991; Potter et al., 1993). However, there are no effective constraints on temperature functions for GPP and ER in these models due to insufficient knowledge about physiological connections. Idealized response functions of (a) plant photosynthesis and ecosystem respiration and (b) net ecosystem production to temperature were illustrated in this study (Fig. 1; Luo, 2007). Gross photosynthesis increases with temperature at its low range, reaches a maximum at optimal temperature, and then declines due to physiology constraints at higher temperatures. Ecosystem respiration consisted of autotrophic and heterotrophic components that increase exponentially with temperature in a very broad range when the respiration rate is mainly limited by biochemical reactions. At the low temperature range, heterotrophic respiration was constrained by substrate supply, and autotrophic respiration always followed the relative constant of GPP, so ecosystem respiration was less than the GPP. Above the optimal temperature of GPP, although the transport of substrates

Table 1
Symbols, definition, unit, initial value and range of parameters that were used in the model-data assimilation.

Parameter	Definition	Unit	Value	Minimum	Maximum	Source
α_q	Canopy quantum efficiency of photon conversion	mol mol^{-1} photon	0.28	0	0.5	1
D_0	Empirical coefficient in Leuning model	kPa	2.74	1	10	2
E_{K_c}	Activation energy of K_c^{25}	J mol^{-1}	59,356	30,000	90,000	1
E_{K_o}	Activation energy of K_o^{25}	J mol^{-1}	35,948	10,000	60,000	1
E_{V_m}	Activation energy of V_m^{25}	J mol^{-1}	58,520	10,000	100,000	1
ER_0	Whole ecosystem respiration at 0 °C	μ mol CO_2 m^{-2} s^{-1}	2.5	1	5	3
$E_{\Gamma_*^{25}}$	Activation energy of CO_2 compensation point at 25 °C	J mol^{-1}	60,000	30,000	100,000	1
f_{ci}	Ratio of internal CO_2 to air CO_2	–	0.87	0.5	0.9	1
g_l	Empirical coefficient in Leuning model	–	1657	100	2000	2
K_n	Canopy extinction coefficient for light		0.8	0.7	0.9	1
K_c^{25}	Michaelis–Menten constant for carboxylation	μ mol mol^{-1}	460	50	600	1
K_c^{25}	Michaelis–Menten constant for oxygenation	mol mol^{-1}	0.33	0.2	0.5	1
Γ_*^{25}	CO_2 compensation point without dark respiration	μ mol mol^{-1}	42.5	10	200	1
$r_{J_mV_m}$	Ratio of J_m to V_m^{25} at 25 °C	–	1.79	1	5	1
Q_{10}	Temperature dependency of ecosystem respiration	–	2	1	3	3
V_m^{25}	Maximum carboxylation rate at 25 °C	μ mol CO_2 m^{-2} s^{-1}	29	10	300	1

1, Knorr and Kattge (2005); 2, van Wijk et al. (2000); and 3, Novick et al. (2004).

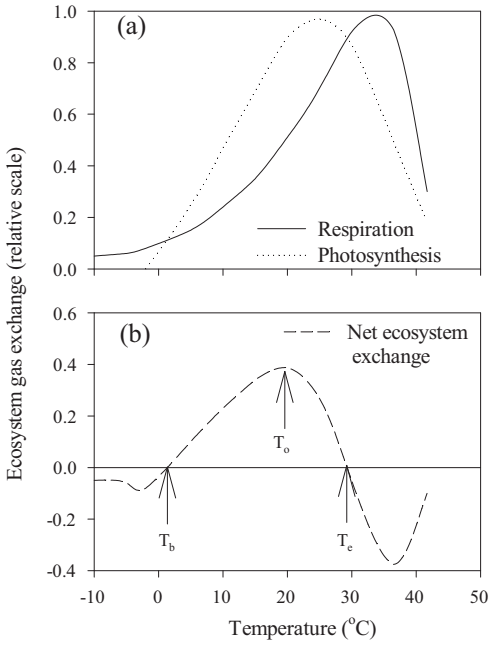

Fig. 1. Idealized response functions of (a) plant photosynthesis and ecosystem respiration and (b) net ecosystem exchange to temperature (Redrawn based on Luo, 2007). Positive values at *y*-axes indicate that carbon is absorbed by the ecosystems, while negative values indicate that carbon is released by the ecosystems to the atmosphere. T_b: transition temperature from ecosystem carbon source to uptake; T_o: optimal temperature of net ecosystem exchange; and T_e: transition temperature from ecosystem carbon uptake to source.

and products of the metabolism mainly via diffusion processes becomes a limiting factor to autotrophic respiration, the abundant supply of substrates promotes the increase in heterotrophic respiration. As a result, ER increases beyond GPP. However, with still further increase in temperature, heterotrophic respiration drops with decreasing substrate supply. During the whole progress, there are two important response temperature points of NEE: the transition temperature from ecosystem carbon source to uptake (T_b) and optimal temperature at which NEE is maximized (T_o) (Fig. 1).

In the previous study, we constructed response curves of NEE against temperature using 380 site-years of eddy covariance data from 72 sites located at latitudes ranging from ~29°N to ~64°N (Yuan et al., 2011). The constructed response curves were used to define two critical temperatures T_b and T_o. The transition temperature T_b was strongly correlated with mean annual air temperature. The optimal temperature T_o was strongly correlated with mean temperature during growing season across the spatial scale (Fig. 2; Yuan et al., 2011). Temperature curves of NEE at Howland were characterized over 9 years, and T_b and T_o shifted to a higher temperature in the warmest year (Fig. 3). The standard deviation of T_b and T_o at Howland are 1.41 °C and 2.10 °C, respectively (Fig. 3).

NEE is the balance between the carbon uptake by photosynthetic carbon uptake and plant and microbial respiratory losses, suggesting that the coupling of two thermally dependent processes should be further examined to evaluate the mechanisms driving thermal adaptation of ecosystem. The thermal adaptation of ecosystem NEE across latitudes suggests the intrinsic physiological connections between thermal responses of GPP and ER, and the responses of GPP and ER to temperature are not independent but coupled (Yuan et al., 2011). Therefore, temperature functions of GPP and ER in these models can be constrained by each other, which will be used in this study to examine the function of the interior coupling relationship between GPP and ER to model parameters inversion.

Our observation regarding T_b was consistent with a previous study by Baldocchi et al. (2005), which showed that net carbon uptake occurs at the period when the mean daily soil temperature equals the mean annual air temperature. Other lines of evidence also support this finding that photosynthesis demonstrates strong correlation with respiration at the ecosystem level (Baldocchi, 2008). The variation of soil respiration and its temperature sensitivity are both strongly correlated with GPP at diurnal, seasonal and annual scales (Janssens et al., 2001; Tang et al., 2005; Ma et al., 2007). Increasing evidence further shows that this complex influence on plant growth rate also determines the microbial processing of carbon in the soil. Chemical properties that promote high physiological activity and growth in plants and low lignin content also promote rapid decomposition (Hobbie, 1992). Furthermore, the quantity of litter input provides a second critical link between CO_2 uptake and decomposition because plant growth governs the quantity of organic matter inputs to decomposers (DeForest, 2009).

2.4. Simulation experiments and statistical analysis

A Bayesian method is used to derive posterior information about model parameters based upon a given set of measurements. According to Bayesian theory, posterior probability density functions (PDFs) of model parameters *c* can be obtained from prior knowledge of parameters and information generated by

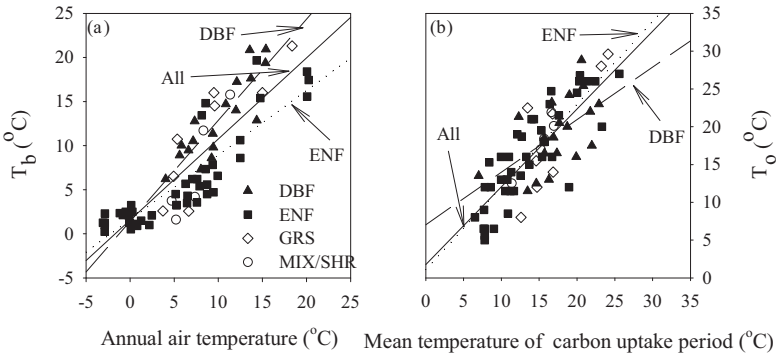

Fig. 2. The relationship between mean annual air temperature vs. T_b (a) and mean temperature of carbon uptake period vs. T_o (b) in deciduous broadleaf forests (DBF), evergreen needleleaf forests (ENF) and all four ecosystems: DBF, ENF, GRS (grasslands), MIX (mixed forests) and SHR (Shurbland). T_b: the transition temperature from ecosystem carbon source to sink; T_o: the optimal temperature for net carbon uptake. At (a), the regression lines are: $y = 1.15x + 1.41$, $R^2 = 0.81$, $P < 0.01$ (DBF); $y = 0.92x + 1.57$, $R^2 = 0.73$, $P < 0.01$ (All); $y = 0.73x + 1.59$, $R^2 = 0.77$, $P < 0.01$ (ENF). At (b), $y = 0.69x + 7.02$, $R^2 = 0.32$, $P < 0.05$ (DBF); $y = 1.02x + 1.76$, $R^2 = 0.64$, $P < 0.01$(All); $y = 1.09x + 1.09$, $R^2 = 0.71$, $P < 0.01$ (ENF).

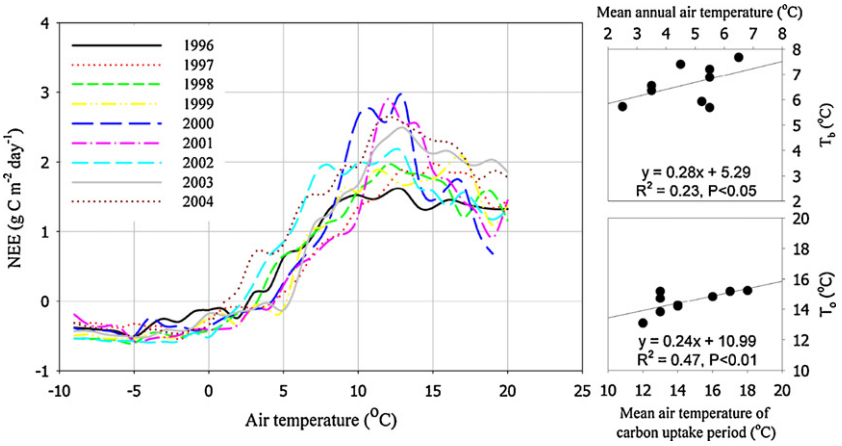

Fig. 3. The temperature curve of net ecosystem exchange at Howland site. The transition temperature from ecosystem carbon source to sink (T_b) and the optimal temperature for net carbon uptake (T_o) were identified from this curve. Positive values at y-axes indicate that carbon is absorbed by the ecosystem, while negative values indicate that that carbon is released by the ecosystem to the atmosphere.

comparison of simulated and observed variables, and can be described as (Mosegaard and Sambridge, 2002):

$$p(c|Z) = \frac{p(Z|c)p(c)}{p(Z)} \tag{2}$$

where $p(c)$ represents prior probability density distributions, $p(Z)$ is the probability of observed data, and $p(Z|c)$ is the conditional probability density of observed data with prior knowledge, also called likelihood function for parameter c. To carry out the data-model assimilation, we first specified ranges for model parameters as prior knowledge (Table 1). The initial values, lower and upper boundaries of parameters, were from Wu et al. (2009) with some modifications on extinction coefficient (K_n) and g_l according to Leuning et al. (1995) and White et al. (2000).

Assuming the errors $e_i(t)$ follow a Gaussian distribution with a zero mean, the likelihood function can be expressed by

$$p(Z|c) \propto \exp\left\{-\sum_i \frac{1}{2\sigma_i^2} \sum_{t \in \text{obs}(Z_i)} (e_i(t))^2\right\} \tag{3}$$

where $e_i(t)$ is the error for each modeled value $Y_i(t)$ compared with the observed value $Z_i(t)$ at time t, expressed by

$$e_i(t) = Z_i(t) - Y_i(t) \tag{4}$$

and σ_i^2 is the measurement error variance of each data set. We assumed that each of elements $e_i(t)$ was independent over the observation times and the covariance is zero, so σ_i^2 was expressed by the variance for each observation data set.

The posterior PDFs for model parameters were generated from prior PDFs $p(c)$ with observations Z by a Markov chain Monte Carlo (MCMC) sampling technique. This study used the Metropolis–Hastings (M–H) algorithm (Metropolis et al., 1953; Hastings, 1970) as the MCMC sampler. Whether a new point c new was accepted or not according to the value of ratio $R = (p(c^{new}|Z)/p(c^{k-1}|Z))$ compared with a uniform random number U from 0 to 1. Only if $R \geq U$, then the new point was accepted; otherwise $c^k = c^{k-1}$ (see Xu et al. (2006) and Zhang et al. (2010) for detailed description on MCMC sampling procedure). We formally made five parallel runs of the M–H algorithm with 20,000 simulations for each run.

We used the Gelman–Rubin (G–R) diagnostic method (Gelman and Rubin, 1992; Xu et al., 2006) and calculated the G–R statistics to examine whether Markov chains converged. The G–R test for each parameter in all experiments satisfied the convergence (G–R statistics approaches to 1) (data not shown). Furthermore, means and standard deviations of posterior parameter sets were approximately stabilized after the first 10,000 samples. Thus, we regarded the first 10,000 times as the burn-in period for each MCMC run. All accepted samples from five runs after burn-in periods (about

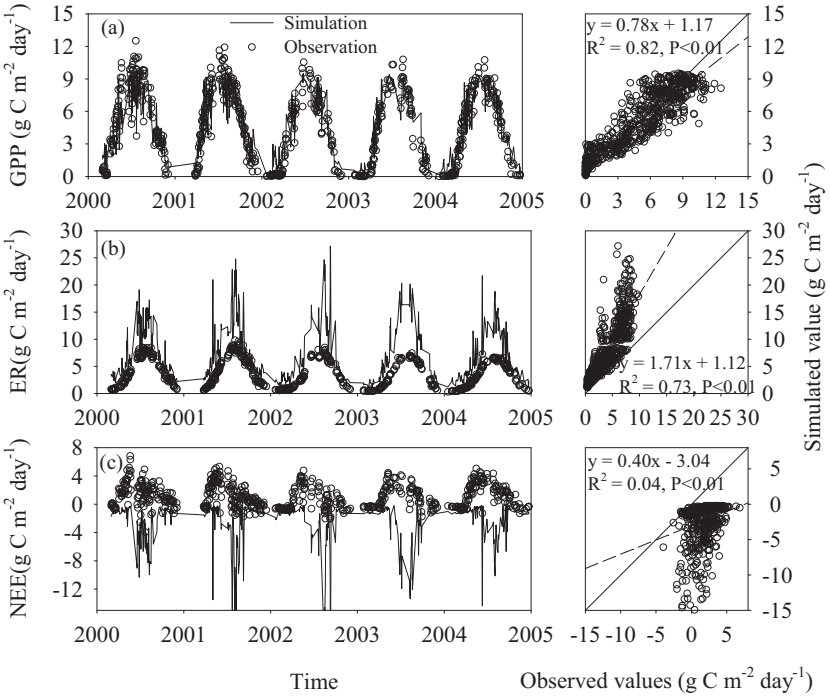

Fig. 4. Comparisons between observed and modeled gross primary production (GPP), ecosystem respiration (ER), and net ecosystem exchange (NEE) at the Howland site after the target parameters listed in Table 1 were optimized using the GPP observations only. For each set of plots, the left and right panels present the comparison in time series and by correlation respectively. At the left panels, the solid lines indicate the simulated GPP, ER, and NEE, and the open dots indicate the observed values. For NEE, the positive values indicate the net ecosystem carbon uptake, and the negative values indicate the net ecosystem carbon release.

50,000 samples) were used to compute posterior parameter statistics of modes, correlations, and 90% confidence intervals.

We designed several simulation experiments to investigate the effectiveness of physiological processes to constrain model parameter estimation via inversion. In the first experiment (experiment 1), we simulated the GPP value through the FBEM model by using the parameter vector generated in the proposing step and then compared the modeled GPP with estimated GPP based on EC measurements. In the second experiment (experiment 2), the probability of accepting new parameters not only depends on model performance for simulating GPP, but also the model fit of T_b and T_o of temperature curves derived from the simulations and observations. In the second experiment, for each model simulation run, temperature curve of NEE was characterized based on NEE simulations, and T_b and T_o determined accordingly. Then, these two temperature points of NEE were compared with those derived from observed data. Similarly, we conducted two other experiments where we used observed NEE data as a substitute for GPP to investigate the effectiveness of co-occurring physiological processes. The third experiment used only observed NEE data (experiment 3), and the fourth experiment also took into account observed NEE data and the model fit of T_b and T_o of temperature curves derived from the simulations and observations (experiment 4). Moreover, the fifth experiment was designed using observed NEE, estimated ER, and estimated GPP data based on EC measurements in a probabilistic inversion (experiment 5). For these model experiments, measurement error variance of each data set was expressed by the standard deviation for each observation data, 1.53 g C m^{-2} d^{-1} for NEE, 3.06 g C m^{-2} d^{-1} for ER, 3.88 g C m^{-2} d^{-1} for GPP, 1.41 °C for T_b and 2.10 °C for T_o (Fig. 3).

Two metrics were used to evaluate the performance of model experiments in this study:

(1) The coefficient of determination, R^2, representing how much variation in the observations was explained by the models.

(2) Relative predictive error (*RPE*), computed as:

$$RPE = \frac{\overline{S} - \overline{O}}{\overline{O}} \times 100\% \quad (5)$$

where $\overline{S}$ and $\overline{O}$ are mean simulated and mean observed values, respectively.

3. Results

We evaluated the performance of MCMC simulations by comparing observed and modeled GPP, ER, and NEE. Figs. 4 and 5 present the simulated GPP, ER, and NEE at the Howland site from the first and second assimilation experiments using estimated GPP based upon EC measurements. The model fitted GPP very well for both of the two experiments, but failed to simulate ER as well as NEE when only GPP observations were used in the first experiment. If model parameters were inferred from GPP data together with physiological processes (the second experiment), the modeled ER and NEE were improved. Relative predictive error (RPE) between modeled and observed GPP, ER, and NEE values was 3.01%, 21.77%, and −58.41% in the second experiment 2, averaging better than 1.87%, 101%, and −324% in the first experiment.

The third and fourth experiments used the observed NEE data in a probabilistic inversion to compare the effectiveness of the interior coupling relationship between GPP and ER. The results showed the model simulated NEE very well for both of the experiments, but failed to fit GPP and ER at the third experiment (Fig. 6). In the fifth experiment, GPP, ER, and NEE were simulated very well using observed NEE as well as the estimated GPP and ER based upon EC measurements (data not shown). The averages for RPE of GPP, ER, and NEE were 2.95%, 16.72%, and 34.61% in the fifth experiment.

Generally, estimated parameters by probabilistic inversion can be divided into three groups: well-constrained, poorly constrained, and edge-hitting depending upon the shape of posterior

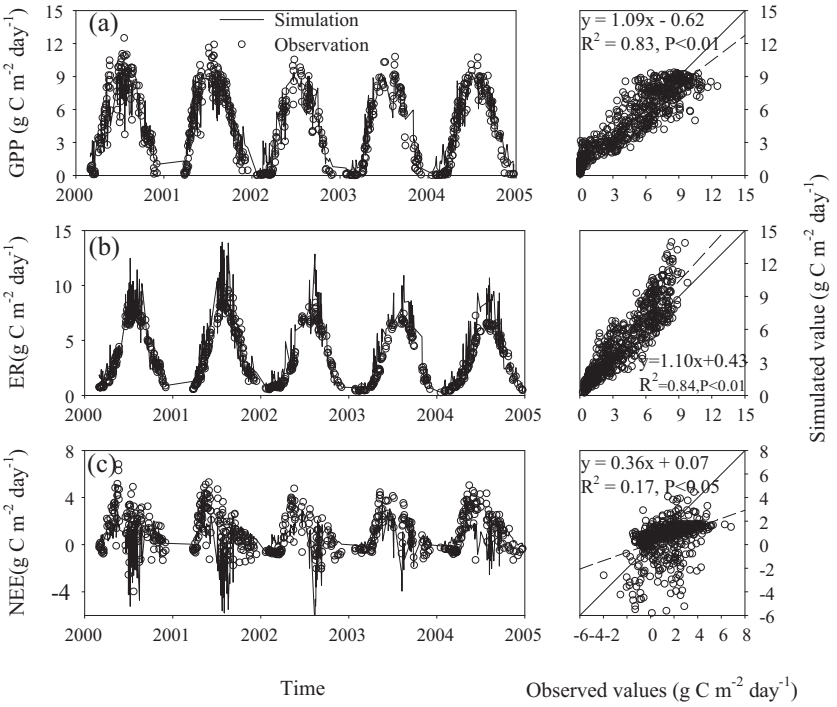

Fig. 5. Comparisons between observed and modeled gross primary production (GPP), ecosystem respiration (ER), and net ecosystem exchange (NEE) (panels a–c) after the target parameters listed in Table 1 were optimized using the GPP observations and the interior connection GPP and ER. For each set of plots, the left and right panels present the comparison in time series and by correlation respectively. For NEE, the positive values indicate the net ecosystem carbon uptake, and the negative values indicate the net ecosystem carbon release.

distributions. In the first experiment, a few of the parameters on GPP (i.e., α_q, $r_{J_mV_m}$, V_m^{25} and E_{V_m}) were well constrained by estimated GPP based on eddy covariance measurements, but both parameters for ecosystem respiration (i.e., ER_0 and Q_{10}) were poorly constrained (Fig. 7). In the second experiment, besides 4 model parameters constrained in the first experiment, another 6 parameters (i.e., Γ_*^{25}, f_{ci}, K_n, $E_{\Gamma_*^{25}}$, ER_0 and Q_{10}) were also well constrained (Fig. 8). The model parameter for ER (ER_0 and Q_{10}) was

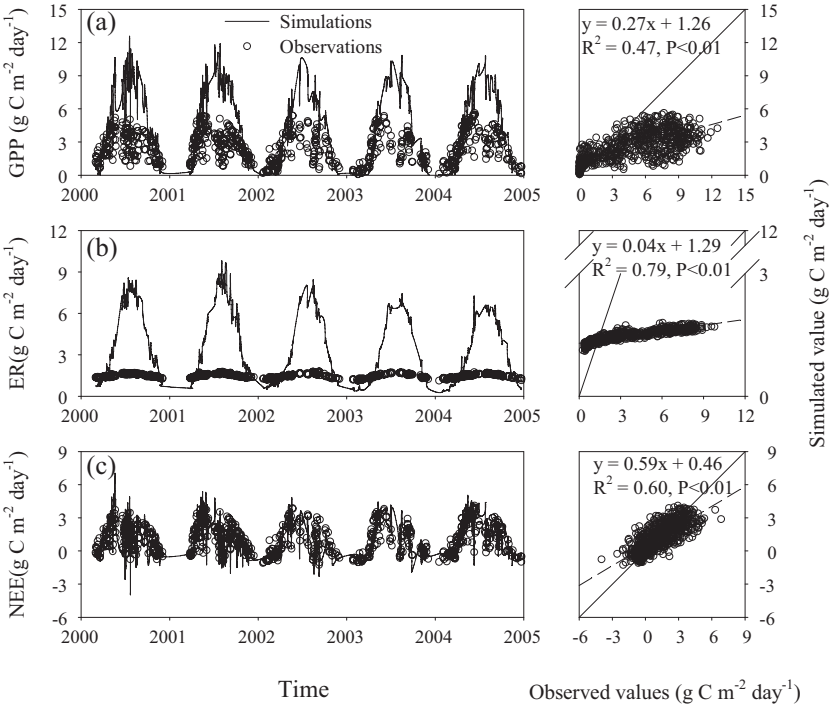

Fig. 6. Comparisons between observed and modeled gross primary production (GPP), ecosystem respiration (ER), and net ecosystem exchange (NEE) (panels a–c) after the target parameters listed in Table 1 were optimized using the NEE observations only at the third experiment. For each set of plots, the left and right panels present the comparison in time series and by correlation respectively. For NEE, the positive values indicate the net ecosystem carbon uptake, and the negative values indicate the net ecosystem carbon release.

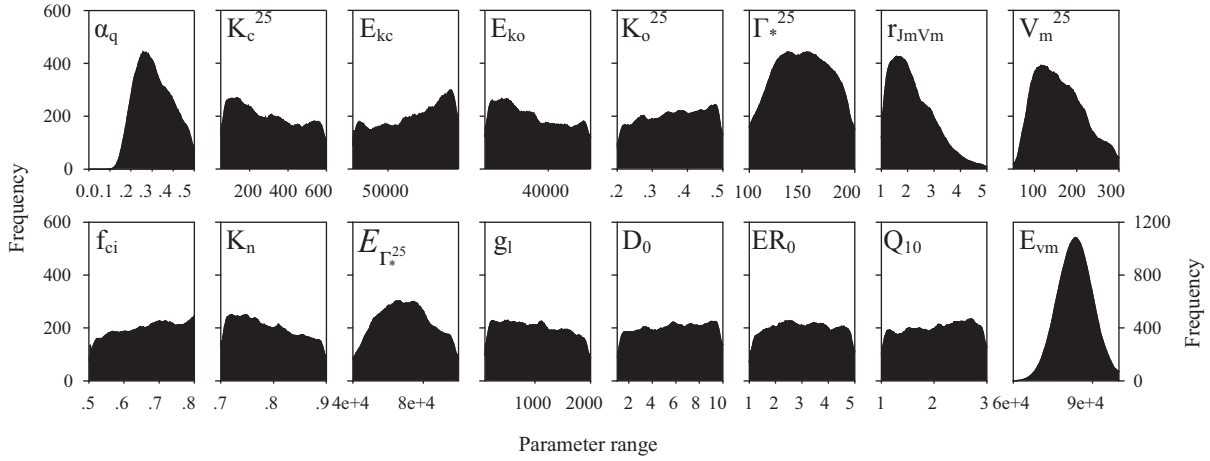

Fig. 7. Histogram to indicate frequency distribution of parameters derived from Bayesian inversion with 100,000 parameter sampling series by the M–H algorithm using the GPP observation only.

especially well constrained in the second experiment without any extra ER observations. Similarly, compared with the third experiment, which only used observed NEE data, the fourth experiment increased greatly the number of constrained parameters by using the relationship between GPP and ER (Table 2). Combining the estimated GPP, ER, and observed NEE data at the fifth experiment, the model constrained up to 13 parameters total (Table 2).

4. Discussion

Many studies have been conducted to improve data assimilation methods in order to increase the number of constrained parameters. Two recent studies (i.e., OptIC and REFLEX project) compared a number of parameter estimation methods applied to common datasets and models (Trudinger et al., 2007). In both the OptIC and REFLEX projects, choices in the implementation of optimization methods, such as data weights, priors, initialization, and method-specific choices such as accept/reject criterion in Metropolis methods, were more important than the choice of the optimization method itself. However, many published studies aim at improving model parameter inversion success by increasing data used (Richardson et al., 2010; Zhang et al., 2010), altering model structures (Chatfield, 1995), and improving optimization methods (Wu et al., 2009). Luo and his colleagues (Luo et al., 2003; Xu et al., 2006), for example, prescribed partitioning coefficients of photosynthates into plant pools, calculating initial values of pool sizes, and using parameters that describe carbon flows into receiving pools in the inverse analysis with six datasets from a forest CO_2 experiment. Here we have used additional constraints on model structure suggested by interior coupling relationships among ecosystem physiological processes.

Our study showed that the coupling relationships between GPP and ER can effectively constrain the parameters on ecosystem respiration without extra observations. In the first model experiment, using GPP observations only, ecosystem respiration parameters (i.e., ER_0 and Q_{10}) could not be constrained; there were large errors in ecosystem respiration simulations when compared with observations from these unreasonable parameters values (Fig. 4). Similarly, the study by Williams et al. (2005) showed respiration parameters to be poorly constrained by NEE measurements alone, and complementary measurements, such as soil respiration and carbon pool sizes provided useful constraints on those parameters. The improved inversion method, using observed GPP and the model fit of T_b and T_o of temperature curves, constrained well the model parameters on ER. Meanwhile, simulated ER agreed very well with observations (Fig. 5). The underlying reason is that the observed GPP and interior relationships among various ecosystem processes limit the acceptable range of ecosystem parameters. At the third experiment, although observed NEE data significantly improved the amount of constrained parameters compared to GPP, the parameters did not fall into the a priori defined "reasonable"

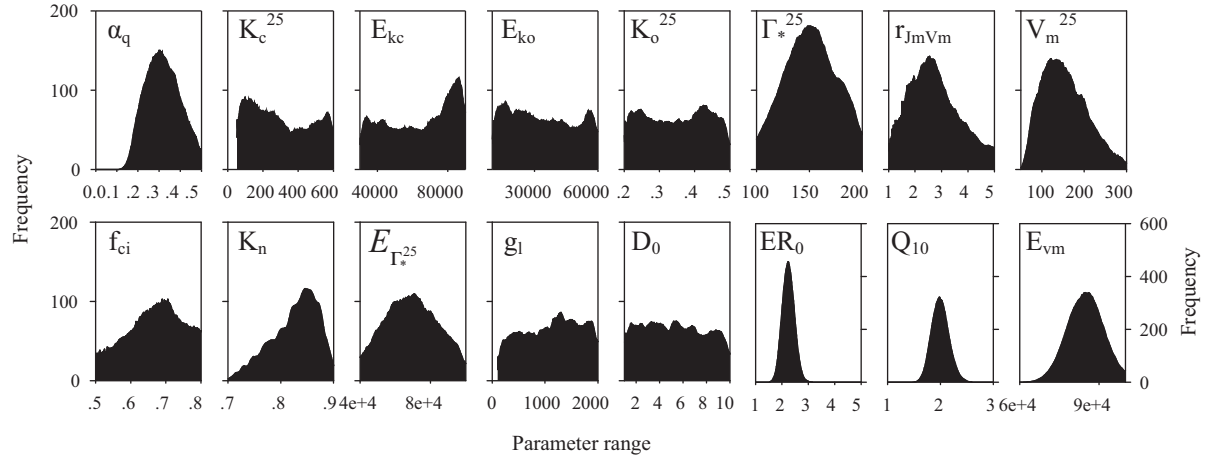

Fig. 8. Histogram to indicate frequency distribution of parameters by the M–H algorithm using the GPP observation and interior connection between GPP and ER.

Table 2
Optimized parameter values at the five model experiments and comparison with parameter ranges published in the literature.

Parameter	Maximum likelihood estimates, mean estimates, 95% high-probability intervals (lower limit, upper limit)					Ranges in literature		Ref.
	First experiment	Second experiment	Third experiment	Fourth experiment	Fifth experiment	Min	Max	
α_q	0.24 [0.31] (0.18–0.46)	0.29 [0.32] (0.19–0.56)	0.05 [0.07] (0.04–0.16)	0.06 [0.05] (0.04–0.08)	0.12 [0.14] (0.10–0.21)	0	0.5	Farquhar et al., 1980; Larcher, 1995; Verbeeck et al., 2006
K_c^{25}	P[a] [300] (78–562)	*P* [304] (77–571)	*P* [287] (83–536)	86.3 [225] (66–508)	E[b] [550] (470–596)	50	600	Bernacchi et al., 2003; Campell and Norman, 1998; Harley and Baldocchi, 1995
E_{K_c}	*P* [63,487] (33,960–87,360)	*P* [63,591] (33,720–87,840)	*P* [57,472] (32,520–86,040)	*P* [59,436] (33,600–85,440)	*E* [85,819] (79,920–89,760)	30,000	90,000	Bernacchi et al., 2003; Harley et al., 1992; Wang et al., 2004
E_{K_o}	*P* [32,683] (12,600–56,800)	*P* [33,846] (12,600–57,300)	*E* [39,131] (14,900–58,300)	*P* [33,320] (12,300–57,400)	13,200 [17,334] (10,800–30,800)	10,000	60,000	Bernacchi et al., 2003; Harley et al., 1992; Wang et al., 2004
K_o^{25}	*P* [0.36] (0.22–0.48)	*P* [0.35] (0.22–0.48)	*P* [0.35] (0.22–0.48)	*P* [0.36] (0.24–0.48)	0.29 [0.27] (0.21–0.42)	0.2	0.5	Bernacchi et al., 2003; von Caemmerer et al., 1994
Γ_*^{25}	*P* [147] (99–190)	146 [148] (102–190)	168 [162] (124–195)	176 [163] (119–195)	23 [39] (13–98)	10	200	Chabot and Mooney, 1985; Larcher, 1995
$r_{Jm}v_m$	1.44 [2.21] (1.17–3.79)	2.44 [2.73] (1.34–4.47)	2.34 [2.89] (1.47–4.68)	2.15 [2.79] (1.30–4.62)	2.48 [2.6] (2.19–3.08)	1	5	Carswell et al., 2000; Wullschleger, 1993
V_m^{25}	134.7 [159] (81–264)	117 [154] (79–251)	188 [192] (99–283)	108 [162] (81–281)	97 [106] (82–139)	10	300	Dreyer et al., 2001; Rey and Jarvis, 1998; Wullschleger, 1993
f_{ci}	*P* [0.71] (0.53–0.87)	0.68 [0.70] (0.53–0.87)	0.65 [0.66] (0.52–0.83)	0.77 [0.73] (0.55–0.87)	0.56 [0.55] (0.50–0.69)	0.5	0.9	Haxeltine et al., 1996; Rey and Jarvis, 1998
K_n	*P* [0.79] (0.71–0.88)	0.84 [0.83] (0.74–0.88)	*E* [0.81] (0.72–0.89)	*P* [0.81] (0.71–0.89)	0.83 [0.85] (0.78–0.89)	0.7	0.9	Larcher, 1995; Wang and Leuning, 1998
$E_{\Gamma_*^{25}}$	*P* [68,880] (42,880–94,820)	69,340 [68,438] (43,020–93,700)	61,086 [63,982] (35,600–93,700)	89,200 [82,351] (57,860–98,180)	40,120 [49,152] (32,380–77,180)	30,000	100,000	Harley et al., 1992; Jordan and Ogren, 1984
g_l	*P* [1001] (210–1859)	*P* [1116] (252–1897)	*P* [1042] (202–1874)	*P* [1045] (248–1867)	*P* [875] (172–1844)	100	2000	–
D_0	*P* [5.65] (1.61–9.49)	*P* [5.33] (1.50–9.37)	*P* [4.75] (1.36–9.29)	4.51 [5.62] (1.86–9.33)	7.98 [7.12] (3.50–9.62)	1	10	–
E_{V_m}	83,800 [83,515] (72,820–94,240)	83,620 [84,729] (73,540–95,680)	95,680 [90,928] (75,880–99,100)	*E* [93,747] (83,620–99,460)	72,460 [73,580] (67,060–80,920)	10,000	100,000	Aalto and Juurola, 2001; Kosugi et al., 2003; Leuning, 1995
ER_0	*P* [3.03] (1.29–4.75)	2.18 [2.24] (1.88–2.62)	1.22 [1.34] (1.07–1.69)	1.51 [1.52] (1.25–1.81)	1.81 [1.83] (1.67–2.00)	1	5	Davidson et al., 2006; Goulden et al., 1996; Hollinger et al., 2004
Q_{10}	*P* [2.03] (1.12–2.88)	1.94 [1.99] (1.74–2.27)	*E* [1.11] (1.01–1.24)	1.12 [1.10] (1.01–1.22)	1.89 [1.90] (1.81–1.99)	1	3	Janssens and Pilegaard, 2003

Values indicate maximum likelihood estimates. Values at square brackets indicate mean estimates and one in parenthesis indicate 95% high-probability intervals (lower limit, upper limit). The first experiment only used GPP data in probabilistic inversion. The second experiment used GPP and temperature adaptation of NEE. The third experiment only NEE observations, and the fourth used NEE and thermal adaptation of NEE. The fifth experiment used GPP, ER and NEE observations.

[a] *P*, poorly constrained parameters.

[b] *E*, edge-hitting parameters.

range of parameters and the model failed to simulate GPP and ER (Fig. 6). Because NEE is the difference between GPP and ER, the model cannot simulate GPP and ER reasonably when aiming at the best NEE match.

Theoretically, the fifth experiment can constrain the largest number of model parameters by integrating the observed NEE as well as the estimated GPP and ER based upon EC measurements, which provides information about GPP, ER, and NEE. The results showed more constrained parameters than other experiments (Table 2). Compared with using the full set of observations, the interior relationship between GPP and ER also provided enough information for constraining model parameters. The second experiment using GPP data and process relationship constrained model parameters very well; the constrained parameters are quite close to those from the fifth experiment, which implied an interior relationship among various ecosystem processes is equivalent with ecosystem observations.

In this study, we used the estimated GPP and ER based upon EC measurements and a simple, statistical model to inversely recover model parameters. Methods to partition NEE to its component fluxes, GPP and ER, have been developed as a way to assess carbon pathways in ecosystems (Reichstein et al., 2005; Stoy et al., 2006). Previous studies have reported that the partitioning method may affect the estimated GPP and ER. For example, when analyzing NEE time series from the same site as the present study, Hagen et al. (2006) reported that GPP estimates for a given year could vary by over 100 g C m^{-2} depending upon the partitioning algorithm (neural network vs. physiologically based) and fitting method (maximum likelihood vs. ordinary least squares) used. More recently Desai et al. (2008) applied 23 different methods to 10 site-years of temperate forest flux data in order to investigate the effects of partitioning method choice on estimated GPP and ER. The results showed that most methods differed by less than 10% in estimating both GPP and ER and were consistent in identifying differences in GPP and ER across sites, which increased confidence in estimated GPP and ER using the current partition methods. The method used in the present study generally performed well when compared with other GPP/ER partitioning approaches (Desai et al., 2008).

Almost all ecosystem physiological processes are linked with others within ecosystems. For example, the ratio of carbon assimilation to transpiration is a function of vapor pressure deficit (VPD), and this function is consistent across the various ecosystem types (Beer et al., 2009). The implication of interior coupling relationships for inverse estimation of model parameters has significant advantages compared with other parameter inversion methods. First, using the interior physiological relationship can effectively reduce the requirements for measuring the various ecosystem variables. The previous studies already showed that the amount and quality of information in the measurements directly determines whether model parameters can be well constrained (Zhang et al., 2010). However, any measurement of ecosystem variables requires time and energy, and some critical ecosystem variables are difficult or impossible to measure.

Second, the interior coupling relationships among ecosystem physiological processes can be easily extrapolated to regional scales from individual sites. Traditionally, model parameter inversion was only conducted at a single site using various observations, and then extrapolated using the parameters to regional and global scales. However, there are large heterogeneities at the spatial patterns of observation sites. For example, the eddy covariance towers, which provide the extensive datasets for net ecosystem exchange of CO_2 (NEE) are biased toward forests, grasslands, and croplands, and are seldom located in deserts or tundra. Geographically, most sites are located in North America, Europe, and East Asia with few sites setup in the Africa and South America.

Lastly, from the regional simulations standpoint, the interior coupling relationships among the various ecosystem physiological processes can improve model performance at regional and global scales. Rayner et al. (2005), using a top-down approach to estimate land surface carbon fluxes, found that 500 surface CO_2 concentration measurements from about 40 monitoring stations per year globally provided little information about model parameters related to leaf photosynthesis or soil carbon turnover rate. An interpretation of the results shows that monthly CO_2 concentrations provide reasonable constraints on the net carbon exchange (i.e., the difference between net primary production and heterotrophic respiration), provided that fluxes from fire, land use change, and so on are well quantified. Little information is available on the atmospheric CO_2 concentration measurements about model parameters related to net primary production and heterotrophic respiration, as the estimates of these two fluxes are often negatively correlated and poorly resolved by surface CO_2 concentration measurements only (Wang and McGregor, 2003). Our study can provide an effective method to improve substantially the estimations of GPP and ER as well as the related model parameters by using the interior coupling relationships among ecosystem processes across the large scales.

5. Summary

Almost all published studies using data assimilation approaches report that the number of parameters that can be constrained is limited. In this study, we examined the function of interior coupling relationship among ecosystem physiological processes on model parameter estimation. The results showed that the coupling relationships between GPP and ER can effectively constrain the parameters relevant to ER without extra observations, and significantly improve model performance for ER as well as NEE. Such improvement in parameter estimation effectively reduced the requirements for the observations of various ecosystem variables, and allowed extrapolation of parameters inversion results to the regional or global scales from the site scale with reduced uncertainty for simulation of carbon dynamics.

Acknowledgements

This research was financially supported by National Key Basic Research and Development Plan of China (2012CB955501 and 2010CB833504), National High Technology Research and Development Program of China (863 Program) (2009AA122101) and the Fundamental Research Funds for the Central Universities. Howland research was supported by the Office of Science (BER), US Department of Energy under Interagency Agreement No. DE-AI02-07ER64355.

Appendix A. Appendix: model structure description

A.1. Leaf-level photosynthesis

Leaf-level photosynthesis was described by a model developed by Farquhar et al. (1980). For C_3 plants, gross leaf CO_2 uptake (A, μmol CO_2 m^{-2} s^{-1}) is calculated as:

$$A = \min\{J_c, J_e\} \tag{A.1}$$

where J_c and J_e represent the rate limited by carboxylation enzymes and by light electron transport, respectively.

The carboxylation processes (J_c, μmol CO_2 m^{-2} s^{-1}) are:

$$J_c = V_m \frac{C_i - \Gamma_*}{C_i + K_c(1 + (O_x/K_o))} \tag{A.2}$$

C_i is the leaf internal CO_2 concentration (μmol CO_2 mol^{-1} air), expressed as

$$C_i = f_{c_i} \times C_a \tag{A.3}$$

with C_a is ambient CO_2 concentration (365 μmol CO_2 mol^{-1} air) and f_{ci} is ratio of leaf internal CO_2 to ambient air CO_2 concentration. O_x is oxygen concentration in the air (0.21 mol O_2 mol^{-1} air). V_m is maximum carboxylation rate (μmol CO_2 m^{-2} s^{-1}), which is related to canopy temperature T_k (K) and activation energy E_{V_m} by Arrhenius' equation:

$$V_m = V_m^{25} \times \exp\left(\frac{E_{V_m} \times (T_k - 298)}{R \times T_k \times 298}\right) \tag{A.4}$$

where V_m^{25} is maximum carboxylation rate at 25 °C and R is universal gas constant (8.314 J K^{-1} mol^{-1}). The CO_2 compensation point without dark respiration is represented as Γ_* (μmol CO_2 mol^{-1}). It is also adjusted by Arrhenius' equation in:

$$\Gamma_* = \Gamma_*^{25} \times \exp\left(\frac{E_{\Gamma_*^{25}} \times (T_k - 298)}{R \times T_k \times 298}\right) \tag{A.5}$$

where Γ_*^{25} is the CO_2 compensation point without dark respiration at 25 °C and $E_{\Gamma_*^{25}}$ describes the temperature dependence of Γ_*. Two Michaelis–Menten constants have a temperature dependence based on the Arrhenius' equation similar to V_m, K_c, Michaelis–Menten constant for carboxylation (μmol mol^{-1}), was represented by:

$$K_c = K_c^{25} \times \exp\left(\frac{E_{K_c} \times (T_K - 298)}{R \times T_K \times 298}\right) \tag{A.6}$$

with an activation energy E_{K_c}, where K_c^{25} is the Michaelis–Menten constant for carboxylation at 25 °C. K_o, Michaelis–Menten constant for oxygenation (mol mol^{-1}), was represented as:

$$K_o = K_o^{25} \times \exp\left(\frac{E_{K_o} \times (T_K - 298)}{R \times T_K \times 298}\right) \tag{A.7}$$

with an activation energy E_{K_o}, where K_o^{25} is the Michaelis–Menten constant for oxygenation at 25 °C.

The light electron transport processes (J_e, μmol CO_2 m^{-2} s^{-1}) are:

$$J_e = \frac{\alpha_q \times I \times J_m}{\sqrt{J_m^2 + \alpha_q^2 \times I^2}} \times \frac{C_i - \Gamma_*}{4 \times (C_i + 2\Gamma_*)} \tag{A.8}$$

when I is absorbed photosynthetically activated radiation (PAR) (μmol m^{-2} s^{-1}). α_q is quantum efficiency of photon capture (mol mol^{-1} photon) and J_m is maximum electron transport rate (μmol CO_2 m^{-2} s^{-1}). J_m depends on temperature and is computed by:

$$J_m = r_{J_m V_m} \times V_m^{25} \times \exp\left(\frac{E_{V_m} \times (T_K - 298)}{R \times T_K \times 298}\right) \tag{A.9}$$

where $r_{J_m V_m}$ is the ratio of J_m to V_m^{25} at 25 °C.

A.2. Stomatal conductance

The stomatal conductance (G_s) is coupled with leaf-level photosynthesis by Leuning model (Leuning, 1995) so that the carbon influx of the top leaf layer (A_n) is estimated by:

$$\begin{aligned} A_n &= G_s \times (C_a - C_i) \\ G_s &= g_l \times \frac{A}{(C_i - \Gamma_*) \times (1 + (D/D_0))} \end{aligned} \tag{A.10}$$

where g_l and D_0 (kPa) are empirical coefficients and D is vapor pressure deficit (kPa).

A.3. Canopy-level photosynthesis

In order to scale up leaf-level photosynthesis to canopy-level photosynthesis, an approach of Sellers et al. (1992) was used to describe the relationship between the canopy photosynthesis (A_c) and the carbon influx of the top leaf layer, derived as:

$$A_c = A_n \times \frac{1 - \exp(-k_n \times LAI)}{k_n} \tag{A.11}$$

where k_n is light extinction coefficient and LAI is leaf area index.

A.4. Ecosystem respiration

Ecosystem respiration (ER) is modeled as a function of temperature (T_a, °C) with the widely used van't Hoff equation (Van't Hoff, 1899):

$$ER = ER_0 \times Q_{10}^{T_a/10} \tag{A.12}$$

where ER_0 us ecosystem respiration at 0 °C and Q_{10} is the relative increase (ER/ER_0) in respiration for every 10 °C rise in temperature.

References

Aalto, T., Juurola, E., 2001. Parametrization of a biochemical CO_2 exchange model for birch (*Betula pendula* Roth). Boreal Environment Research 6, 53–64.

Ågren, G.I., Bosatta, E., 1998. Theoretical Ecosystem Ecology – Understanding Element Cycles. Cambridge Univeristy Press, Cambridge.

Baldocchi, D.D., 2008. 'Breathing' of the terrestrial biosphere: lessons learned from a global network of carbon dioxide flux measurement systems. Australian Journal of Botany 56, 1–26.

Baldocchi, D.D., Black, T.A., Curtis, P., Falge, E., Fuentes, J.D., Granier, A., Gu, L., Knohl, A., Lee, X., Pilegaard, K., Schmid, H.P., Valentini, R., Wofsy, S., Xu, L., Yamamoto, S., 2005. Predicting the onset of carbon uptake by deciduous forests with soil temperature and climate data: a synthesis of FLUXNET data. International Journal of Biometeorology 49, 377–387.

Beer, C., Ciais, P., Baldocchi, D., Law, B.E., Papale, D., Soussana, J.F., Ammann, C., Buchmann, N., Frank, D., Gianelle, D., Janssens, I.A., Knohl, A., Köstner, M.E., Roupsard, O., Verbeeck, H., Vesasla, T., Williams, C.A., Wohlfahrt, G., 2009. Temporal and among-site variability of inherent water use efficiency at the ecosystem level. Global Biogeochemical Cycles 23, GB2018, http://dx.doi.org/10.1029/2008GB003233.

Bernacchi, C.J., Pimentel, C., Long, S.P., 2003. In vivo temperature response functions of parameters required to model RuBP-limited photosynthesis. Plant, Cell & Environment 26, 1419–1430.

Braswell, B.H., Sacks, W.J., Linder, E., Schimel, D.S., 2005. Estimating diurnal to annual ecosystem parameters by synthesis of a carbon flux model with eddy covariance net ecosystem exchange observations. Global Change Biology 11, 335–355.

Campell, G.S., Norman, J.M., 1998. An Introduction to Environmental Biophysics. Springer, New York.

Carswell, F.E., Meir, P., Wandelli, E.V., Bonates, L.C.M., Kruijt, B., Barbosa, E.M., Nobre, A.D., Grace, J., Jarvis, P.G., 2000. Photosynthetic capacity in a central Amazonian rain forest. Tree Physiology 20, 179–186.

Chabot, B.F., Mooney, H.A., 1985. Physiological Ecology of North American Plant Communities. Chapman and Hall, New York.

Chang, M., 2003. Forest Hydrology. An Introduction to Water and Forests. CRC Press, Washington, DC.

Chatfield, C., 1995. Model uncertainty, data mining and statistical-inference. Journal of the Royal Statistical Society Series A: Statistics in Society 158, 419–466.

Davidson, E.A., Richardson, A.D., Savage, K.E., Hollinger, D.Y., 2006. A distinct seasonal pattern of the ratio of soil respiration to total ecosystem respiration in a spruce-dominated forest. Global Change Biology 12, 230–239.

DeForest, J.L., 2009. The influence of time, storage temperature, and substrate age on potential soil enzyme activity in acidic forest soils using MUB-linked substrates and L-DOPA. Soil Biology and Biochemistry 41, 1180–1186.

Desai, A.R., Richardson, A.D., Moffat, A.M., Kattge, J., Hollinger, D.Y., Barr, A., Flage, E., Noormets, A., Papale, D., Reichstein, M., Stauch, V.J., 2008. Cross site evaluation of eddy covariance GPP and RE decomposition techniques. Agricultural and Forest Meteorology 148, 821–838.

Dreyer, E., Le Roux, X., Montpied, P., Daudet, F.A., Masson, F., 2001. Temperature response of leaf photosynthetic capacity in seedlings from seven temperate tree species. Tree Physiology 21, 223–232.

Farquhar, G.D., Von Caemmerer, S., Berry, J.A., 1980. A biochemical model of photosynthesis in leaves of C3 species. Planta 149, 78–90.

Gelman, A., Rubin, D.B., 1992. Inference from iterative simulation using multiple sequences. Statistical Science 7, 457–511.

Goulden, M.L., Munger, J.W., Fan, S.M., Daube, B.C., Wofsy, S.C., 1996. Measurements of carbon sequestration by long-term eddy covariance: methods and a critical evaluation of accuracy. Global Change Biology 2, 169–182.

Gove, J.H., Hollinger, D.Y., 2006. Application of a dual unscented Kalman filter for simultaneous state and parameter estimation in problems of surface-atmosphere exchange. Journal of Geophysical Research 111, D08S07, http://dx.doi.org/10.1029/2005JD006021.
Green, E.J., MacFarlane, D.W., Valentine, H.T., Strawderman, W.E., 1999. Assessing uncertainty in a stand growth model by Bayesian synthesis. Forensic Science 45, 528–538.
Hagen, S.C., Braswell, B.H., Linder, E., Frolking, S., Richardson, A.D., Hollinger, D.Y., 2006. Statistical uncertainty of eddy flux-based estimates of gross ecosystem carbon exchange at Howland Forest, Maine. Journal of Geophysical Research 111, D08S03, http://dx.doi.org/10.1029/2005JD006154.
Harley, P.C., Baldocchi, D.D., 1995. Scaling carbon-dioxide and water vapor exchange from leaf to canopy in a deciduous forest. 1. Leaf model parametrization. Plant Cell and Environment 18, 1146–1156.
Harley, P.C., Thomas, R.B., Reynolds, J.F., Strain, B.R., 1992. Modelling photosynthesis of cotton grown in elevated CO_2. Plant, Cell and Environment 15, 271–282.
Hastings, W.K., 1970. Monte Carlo sampling methods using Markov chain and their applications. Biometrika 57, 97–107.
Haxeltine, A., Prentice, I.C., Creswell, D.I., 1996. A coupled carbon and water flux model to predict vegetation structure. Journal of Vegetation Science 7, 651–666.
Hobbie, S., 1992. Effects of plant species on nutrient cycling. Trends in Ecology and Evolution 7, 336–339.
Hollinger, D.Y., Richardson, A.D., 2005. Uncertainty in eddy covariance measurements and its application to physiological models. Tree Physiology 25, 873–885.
Hollinger, D.Y., Aber, J., Dail, B., Davidson, E.A., Goltz, S.M., Hughes, H., Leclerc, M.Y., Lee, J.T., Richardson, A.D., Rodrigues, C., Scott, N.A., Achuatavarier, D., Walsh, J., 2004. Spatial and temporal variability in forest-atmosphere CO_2 exchange. Global Change Biology 10, 1689–1706.
Hollinger, D.Y., Goltz, S.M., Davidson, E.A., Lee, J.T., Tu, K., Valentine, H.T., 1999. Seasonal patterns and environmental control of carbon dioxide and water vapour exchange in an ecotonal boreal forest. Global Change Biology 5, 891–902.
Janssens, I.A., Kowalski, A.S., Ceulemans, R., 2001. Forest floor CO_2 fluxes estimated by eddy covariance and chamber-based model. Agricultural and Forest Meteorology 106, 61–69.
Janssens, I.A., Pilegaard, K., 2003. Large seasonal changes in Q_{10} of soil respiration in a beech forest. Global Change Biology 9, 911–928.
Jordan, D.B., Ogren, W.L., 1984. The CO_2/O_2 specificity of ribulose-1,5-bisphorphate carboxylase/oxygenase: dependence on ribulose bisphosphate concentration, PH, and temperature. Planta 161, 308–313.
Knorr, W., Kattge, J., 2005. Inversion of terrestrial ecosystem model parameter values against eddy covariance measurements by Monte Carlo sampling. Global Change Biology 11, 1333–1351.
Kosugi, Y., Shibata, S., Kobashi, S., 2003. Parameterization of the CO_2 and H_2O gas exchange of several temperate deciduous broad-leaved trees at the leaf scale considering seasonal changes. Plant, Cell and Environment 26, 285–301.
Larcher, W., 1995. Physiological Plant Ecology: Ecophysiology and Stress Physiology of Functional Groups. Springer, Berlin.
Leuning, R., 1995. A critical appraisal of a combined stomatalphotosynthesis model for C3 plants. Plant, Cell and Environment 18, 339–356.
Leuning, R., Kelliher, F.M., De Pury, D.G.G., Schulze, E.D., 1995. Leaf nitrogen, photosynthesis, conductance and transpiration: scaling from leaves to canopies. Plant Cell and Environment 18, 1183–1200.
Luo, Y.Q., 2007. Terrestrial carbon cycle feedback to climate warming. Annual Review of Ecology, Evolution, & Systematics 38, 683–712.
Luo, Y.Q., Wu, L.H., Andrews, J.A., White, L., Matamala, R., Schäfer, K.V.R., Schlesinger, W.H., 2001. Elevated CO_2 differentiates ecosystem carbon processes: deconvolution analysis of Duke Forest FACE data. Ecological Monographs 71, 357–376.
Luo, Y.Q., White, L.W., Canadell, J.G., DeLucia, E.H., Ellsworth, D.S., Finzi, A., Lichter, J., Schlesinger, W.H., 2003. Sustainability of terrestrial carbon sequestration: a case study in Duke Forest with inversion approach. Global Biogeochemical Cycles 17, 1021, http://dx.doi.org/10.1029/2002GB001923.
Ma, S., Baldocchi, D.D., Xu, L., Hehn, T., 2007. Interannual variability in carbon exchange of an oak/grass savanna and an annual grassland in California. Agricultural and Forest Meteorology 147, 157–171.
MacFarlane, D.W., Green, E.J., Valentine, H.T., 2000. Incorporating uncertainty into the parameters of a forest process model. Ecological Modelling 134, 27–40.
Metropolis, N., Rosenbluth, A.W., Rosenbluth, M.N., Teller, A.H., Teller, E., 1953. Equation of state calculation by fast computing machines. Journal of Chemical Physics 21, 1087–1092.
Mosegaard, K., Sambridge, M., 2002. Monte Carlo analysis of inverse problems. Inverse Problems 18, 29–54.
Novick, K.A., Stoy, P.C., Katul, G.G., Ellsworth, D.S., Siqueira, M.B.S., Juang, J., Oren, R., 2004. Carbon dioxide and water vapor exchange in a warm temperate grassland. Oecologia 138, 259–274.
Odum, H.T., 1956. Primary production in flowing waters. Limnology and Oceanography 1, 102–117.
Parton, W.J., Schimel, D.S., Cole, C.V., Ojima, D.S., 1987. Analysis of factors controlling soil organic-matter levels in Great-Plains grasslands. Soil Science Society of America Journal 51, 1173–1189.
Potter, C.B., Randerson, J.T., Field, C.B., Matson, P.A., Vitousek, P.M., Mooney, H.A., Klooster, S.A., 1993. Terrestrial ecosystem production: a process model based on global satellite and surface data. Global Biogeochemical Cycles 7, 811–841.
Rastetter, E.B., Ryan, M.G., Shaver, G.R., Melillo, J.M., Nadelhoffer, K.J., Hobbie, J.E., Aber, J.D., 1991. A general biogeochemical model describing the response of the C and N cycles in terrestrial ecosystems to changes in CO_2, climate, and N deposition. Tree Physiology 9, 101–126.
Raupach, M.R., Rayner, P.J., Barrett, D.J., Defries, R.S., Heimann, M., Ojima, D.S., Quegan, S., Schmullius, C.C., 2005. Model-data synthesis in terrestrial carbon observation: methods, data requirements and data uncertainty specifications. Global Change Biology 11, 378–397.
Rayner, P., Scholze, M., Knorr, W., Kaminski, T., Giering, R., Widmann, H., 2005. Two decades of terrestrial carbon fluxes from a carbon cycle data assimilation system (CCDAS). Global Biogeochemical Cycles 19, http://dx.doi.org/10.1029/2004GB002254.
Reichstein, M., Falge, E., Baldocchi, D., 2005. On the separation of net ecosystem exchange into assimilation and ecosystem respiration: review and improved algorithm. Global Change Biology 11, 1–16.
Rey, A., Jarvis, P.G., 1998. Long-term photosynthetic acclimation to increased atmospheric CO_2 concentration in young birch (*Betula pendula*) trees. Tree Physiology 18, 441–450.
Richardson, A.D., Williams, M., Hollinger, D.Y., Moore, D.J.P., Dail, D.B., Davidson, E.A., Scott, N.A., Evans, R.S., Hughes, H., Lee, J.T., Rodrigues, C., Savage, K., 2010. Estimating parameters of a forest ecosystem C model with measurements of stocks and fluxes as joint constraints. Oecologia 164, 25–40.
Richardson, A.D., Braswell, B.H., Hollinger, D.Y., Burman, P., Davidson, E.A., Evans, R.S., Flanagan, L.B., Munger, J.W., Savage, K., Urbanski, S.P., Wofsy, S.C., 2006. Comparing simple respiration models for eddy flux and dynamic chamber data. Agricultural and Forest Meteorology 141, 219–234.
Running, S.W., Coughlan, J.C., 1998. A general model of forest ecosystem processes for regional applications, I. Hydrologic balance, canopy gas exchange and primary production processes. Ecological Modelling 42, 125–154.
Running, S.W., Gower, S.T., 1991. FOREST-BGC a general model of forest ecosystem processes for regional applications, II. Dynamic carbon allocation and nitrogen budgets. Tree Physiology 9, 147–160.
Santaren, D., Peylin, P., Viovy, N., Ciais, P., 2007. Optimizing a process-based ecosystem model with eddy-covariance flux measurements: a pine forest in southern France. Global Biogeochemical Cycles 21, GB2013, http://dx.doi.org/10.1029/2006GB002834.
Schulz, K., Jarvis, A., Beven, K., Soegaard, H., 2001. The predictive uncertainty of land surface fluxes in response to increasing ambient carbon dioxide. Journal of Climate 14, 2551–2562.
Sellers, P.J., Berry, J.A., Collatz, G.J., Field, C.B., Hall, F.G., 1992. Canopy reflectance, photosynthesis, and transpiration. III. A reanalysis using improved leaf models and a new canopy integration scheme. Remote Sensing of Environment 42, 187–216.
Stoy, P.C., Katul, G.G., Siqueira, M.B.S., Juang, J.Y., Novick, K.A., Oren, R., 2006. An evaluation of methods for partitioning eddy covariance-measured net ecosystem exchange into photosynthesis and respiration. Agricultural and Forest Meteorology 141, 2–18.
Tang, J., Baldocchi, D.D., Xu, L., 2005. Tree photosynthesis modulates soil respiration on a diurnal time scale. Global Change Biology 11, 1298–1304.
Trudinger, C.M., Raupach, M.R., Rayner, P.J., Kattge, J., Liu, Q., Pak, B., Reichstein, M., Renzullo, L., Richardson, A.D., Roxburgh, S.H., Styles, J., Wang, Y.P., Briggs, P., Barrett, D., Nikolova, S., 2007. OptIC project: an intercomparison of optimization techniques for parameter estimation in terrestrial biogeochemical models. Journal of Geophysical Research 112, G02027, http://dx.doi.org/10.1029/2006JG000367.
Van Oijen, M., Rougier, J., Smith, R., 2005. Bayesian calibration of process-based forest models: bridging the gap between models and data. Tree Physiology 25, 915–927.
van Wijk, M.T., Dekker, W.S.C., Bosveld, F.C., Kohsiek, W., Kramer, K., Mohren, G.M., 2000. Modeling daily gas exchange of a Douglas-fir forest: comparison of three stomatal conductance models with and without a soil water stress function. Tree Physiology 20, 115–122.
Van't Hoff, J.H., 1899. Lectures on Theoretical and Physical Chemistry. Edward Arnold, London.
Verbeeck, H., Samson, R., Verdonck, F., Raoul, L., 2006. Parameter sensitivity and uncertainty of the forest carbon flux model FORUG: a Monte Carlo analysis. Tree Physiology 26, 807–817.
von Caemmerer, S., Evans, J.R., Hudson, G.S., 1994. The kinetics of ribulose-1,5-biosphosphate caboxylase/oxygenase in vivo inferred from measurements of photosynthesis in leaves of ransgenic tobacco. Planta 195, 88–97.
Wang, Q., Tenhunen, J., Falge, E., Bernhofer Ch, Granier, A., Vesala, T., 2004. Simulation and scaling of temporal variation in gross primary production for coniferous and deciduous temperate forests. Global Change Biology 10, 37–51.
Wang, Y.P., Barrett, D.J., 2003. Estimating regional terrestrial carbon fluxes for the Australian continent using a multiple-constraint approach, I. Using remotely sensed data and ecological observations of net primary production. Tellus 55B, 270–289.
Wang, Y.P., McGregor, J.L., 2003. Estimating regional terrestrial carbon fluxes for the Australian continent using a multiple-constraint approach, II. The atmospheric constraint. Tellus 55B, 290–304.
Wang, Y.P., Leuning, R., 1998. A two-leaf model for canopy conductance, photosynthesis and partitioning of available energy, I: model description and comparison with a multi-layered model. Agricultural and Forest Meteorology 91, 89–111.
Wang, Y.P., Leuning, R., Cleugh, H.A., Coppin, P.A., 2001. Parameter estimation in surface exchange models using nonlinear inversion: how many parameters can we estimate and which measurements are most useful? Global Change Biology 7, 495–510.
Watt, K.E.F., 1966. Systems Analysis in Ecology. McGraw-Hill Book Co, New York.

Weng, E.S., Luo, Y.Q., 2007. Uncertainty analysis with data-model assimilation at Duke FACE. In: National Science Foundation workshop "Data-Model Assimilation in Ecology: Techniques and Applications", Norman, Oklahoma, USA.

White, M.A., Thornton, P.E., Running, S.W., Nemani, R.R., 2000. Parameterization and sensitivity analysis of the BIOME-BGC terrestrial ecosystem model: net primary production controls. Earth Interactions 4, 3–10.

Williams, M., Schwarz, P.A., Law, B.E., Irvine, J., Karpius, M.R., 2005. An improved analysis of forest carbon dynamics using data assimilation. Global Change Biology 11, 89–105.

Wu, X.W., Luo, Y.Q., Weng, E.S., White, L., Ma, Y., Zhou, X.H., 2009. Conditional inversion to estimate parameters from eddy-flux observations. Journal of Plant Ecology 2, 55–68.

Wullschleger, S.D., 1993. Biochemical limitations to carbon assimilation in C3 plants – a retrospective analysis of the A/Ci curves from 109 species. Journal of Experimental Botany 44, 907–920.

Xu, T., White, L., Hui, D., Luo, Y.Q., 2006. Probabilistic inversion of a terrestrial ecosystem model: analysis of uncertainty in parameter estimation and model prediction. Global Biogeochemical Cycles 20, GB2007.

Yuan, W., Luo, Y., Richardson, A., Oren, R., Luyssaert, S., Janssens, I., Ceulemans, R., Zhou, X., Grünwald, T., Aubinet, M., Berhfer, C., Baldocchi, D., Chen, J., Dunn, A., Deforest, J., Dragoni, D., Goldstein, A., Moors, E., Munger, J., Monson, R., Suyker, A., Starr, G., Scott, R., Tenhunen, J., Verma, S., Vesala, T., Wofsy, S., 2009. Latitudinal patterns of magnitude and interannual variability in net ecosystem exchange regulated by biological and environmental variables. Global Change Biology 15, 2905–2920.

Yuan, W., Luo, Y., Liang, S., Liu, S., Yu, G., Niu, S., Stoy, P., Chen, J., Desai, A.R., Lindroth, A., Gough, C.M., Ceulemans, R., Arain, A., Bernhofer, C., Cook, B., Cook, D.R., Dragoni, D., Gielen, B., Janssens, I., Longdoz, B., Liu, H., Lund, M., Matteucci, G., Moors, E., Scott, R.L., Seufert, G., Varner, R., 2011. Thermal adaptation of net ecosystem exchange. Biogeosciences 8, 1453–1463.

Zhang, L., Luo, Y.Q., Yu, G.R., Zhang, L.M., 2010. Estimated carbon residence times in three forest ecosystems of eastern China: applications of probabilistic inversion. Journal of Geophysical Research 115, G01010, http://dx.doi.org/10.1029/2009JG001004.